DOI 10.1007/s11595-015-1224-4

Chemical Composition and Microstructure of Hydration Products of Hardened White Portland Cement Pastes Containing Admixtures

LI Qiu[1,2]

(1.State Key Laboratory of Silicate Materials for Architectures, Wuhan University of Technology, Wuhan 430070, China;2. WUT-UC Berkeley Joint Laboratory on Concrete Science and Technology, Wuhan University of Technology, Wuhan 430070, China)

Abstract: This study investigated the nature of hydration products of white portland cement (WPC) containing 20 mM malic acid or 1 M calcium chloride hydrated for 11 years. The study identified the hydration products and characterized the chemical composition, morphology, micro/nano structure of C-S-H and the main binding phase in cementitious materials. Calcium hydroxide (CH), ettringite and C-S-H were identified in WPC with 20 mM malic acid paste hydrated for 11 years. WPC with 1 M calcium chloride paste hydrated for 11 years contained the same phases, but with less CH, and the presence of Friedel's salt ($Ca_2Al(OH)_6Cl{\cdot}2H_2O$). There were still small amount of anhydrous cement particles remaining in both pastes after 11 years hydration according to the SEM and ^{29}Si MAS NMR results. The hydration products of paste containing malic acid had a lower porosity than those prepared with calcium chloride upon visual inspection under SEM. The morphology of the outer product (Op) C-S-H was coarse fibrillar and the inner product (Ip) C-S-H had a very fine microstructure in both pastes under TEM. Both Ip and Op C-S-H formed in paste containing malic acid had lower Ca/Si and higher Al/Si than those in paste containing calcium chloride. C-S-H in paste containing calcium chloride had longer MCL and less percentage of bridging tetrahedra occupied by aluminum in silicon/aluminum chains due to relatively less Q^1 and more Q^2. A new type of silicon tetrahedra, Q^{2B}, was introduced during deconvolution of ^{29}Si MAS NMR results. Ip and Op C-S-H in both pastes had aluminum substituted tobermorite-type and jennite-type structure, and all the charges caused by aluminum substituting silicon bridging tetrahedra were balanced by Ca^{2+}.

Key words: calcium chloride; malic acid; calcium-silicate-hydrate (C-S-H); TEM; NMR

1 Introduction

The microstructure and composition of hydration products of Portland cement are vital for defining the properties of hardened cement and concrete. The main hydration products are calcium silicate hydrate gels (C-S-H gels), calcium hydroxide (CH) aluminate/aluminoferrite phases (AFt and AFm type phases)[1]. Among these hydration products, the most important one is C-S-H gel because it is the principal binding phase in cement-based systems-responsible for strength, density, *etc*[2]. Its morphology, microstructure and chemical composition define the final properties of the hardened cement. Numerous studies have been done on the nature of C-S-H in hardened cement pastes since the 1950s but its structure is still not fully understood.

Calcium chloride is a well-known accelerator for cement hydration. An early study on its influence on hydration of tricalcium silicate (C_3S) suggested the formation of both foil-like and fibrillar C-S-H[3]. A lot of work has been done since then but the mechanism of acceleration is still unclear[4-7]. Juenger and Peterson suggested that the early age hydration products, which formed around the C_3S particles, were flocculated to increase the diffusion rates of ions and water on the existence of calcium chloride, resulting in the acceleration of hydration of inner products[8,9]. The hydration products had lower density compared to the control. Wilding characterized the effects of a range of inorganic and organic admixtures on cement hydration. The mechanism of the acceleration and retardation of the hydration was discussed, which concluded that retardation was a result of preferential complexation

(Received: Aug. 20, 2014; Accepted: Nov. 10, 2014)

LI Qiu(李秋): Ph D; Assoc. Researcher; E-mail: Qiu.Li@outlook.com

of Ca or Si in solution or C-S-H gel after retarder was added[10].

Malic acid is a known retarder for cement hydration, believed not to alter the mechanism of cement hydration[11]. The retardation mechanism could be due to the absorption of malic acid on the cement particles preventing diffusion of ions and water[12]. Wang reported a morphology change in the hydration products of calcium phosphate cement when malic acid was added but there was no new hydration products formed[13]. Rai meanwhile did report the formation of a new hydration product but this was contradicted by other researchers[11,13,14].

In this study, white portland cement mixed with either an accelerator (calcium chloride) or retarder (malic acid) was studied. The aim of the study was to characterize by various analytical techniques, the hydration products of mature white portland cement containing different admixtures.

2 Experimental

2.1 Materials

The oxide composition of white portland cement used is shown in Table 1. Note that these data were obtained by quantitative XRF so the sulphur content is not shown, however the presence of AFm and AFt phases in the hydration products indicates that there is sulphur in the samples. Calcium chloride ($CaCl_2$•$6H_2O$) and malic acid ($C_4H_6O_5$) were used as admixtures at concentrations of 1 M and 20 mM, respectively.

2.2 Specimen preparation and experimental details

The required amount of white Portland cement was hand-mixed with either calcium chloride (1M) or malic acid (20 mM) solution with a solution/solid (*s/s*) ratio of 0.5. The slurries were then placed in plastic tubes which were sealed in plastic bags before placing in a water bath set at 25 ℃. The samples were well kept and maintained in the water bath before transferred for analysis. The pastes in this study were hydrated approximately for 11 years before being taken for analysis. Freshly ground samples were used for X-ray diffraction (XRD), magic angle spinning nuclear magnetic resonance (MAS NMR) and simultaneous thermal analysis and evolved gas analysis (STA-EGA).

For MAS NMR, specimens were ground and packed into 6 mm zirconia rotors before ^{29}Si and ^{1}H-^{29}Si cross polarization (CP) spectra were acquired by a Varian InfinitePlus-300 spectrometer. The single pulse spectra were acquired over 30000 scans using pulse delays (2s) sufficient to minimize the saturation of the hydration peaks. All spectra were apodized with 10 Hz of exponential line broadening and zero filled to 8192 points prior to Fourier transformation. The spectra were fitted to voigt line shapes using the software Igor Pro with additional macros written by Brough[15].

Table 1 Oxide composition of white Portland cement used in this study. Sulphur is not shown due to the quantitative XRF

Oxides	Percentage/%
SiO_2	25.00
TiO_2	0.08
Al_2O_3	2.14
Fe_2O_3	0.36
Mn_3O_4	0.02
MgO	0.78
CaO	71.02
Na_2O	<0.30
K_2O	0.09
P_2O_5	0.08
Cr_2O_3	<0.01
Total	99.57
LOI* (at 1025 ℃)	1.06

* LOI - Loss on ignition

XRD analysis was performed on finely ground fresh samples packed into sample holder before scanning over the range of 2θ from 6° to 55° with a step of 0.02° by a Philips Analytical X'Pert PRO MRD.

Thermal analysis was performed on samples of about 16 mg, freshly ground and placed into crucible for STA-EGA test, where the sample was heated to 1000 ℃ at a rate of 20 ℃/min.

For SEM, the hydrated samples were cut into 3 mm thick slices and then the hydration was stopped by immersion in isopropanol before being embedded in resin, then polished and coated with carbon. The backscattered electron (BSE) images were taken by Philips XL30 ESEM, under the conditions of spotsize 5, magnification 1000×, and accelerating voltage 20 kV.

For TEM, hydration stopped samples were hand thinned before put into a low angle ion milling system (Agar Model 1010) to prepare TEM samples[16]. TEM was performed by a Philips CM20 under the conditions of spotsize 1, magnification 19500×, accelerating voltage 20 kV for images, and spotsize 3, magnification 15000× for EDX under bright field mode. Images were taken on the negative films, then processed and scanned to digital images. Selected area electron diffraction (SAED) was performed before EDX to eliminate the possible phase intermixing in the examining area.

3 Results and discussion

3.1 Hydration products

XRD analysis revealed Portlandite, ettringite and C-S-H in the retarded paste (Fig.1 (a)). Meanwhile Portlandite, ettringite, C-S-H and hydrocalumite (Friedel's salt) were observed in accelerated paste (Fig.1 (b)). The peaks for Portlandite and ettringite in the retarded paste were more intense than those in calcium chloride paste, indicating that more CH and AFt formed in the former. This was confirmed by STA-EGA results, shown later.

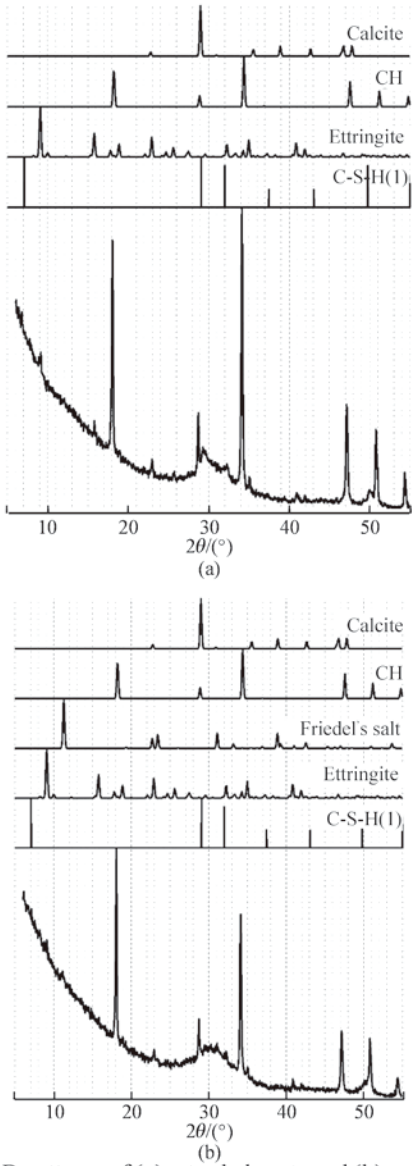

Fig.1 XRD patterns of (a) retarded paste and (b) accelerated paste. Typical peaks of CH, ettringite (peaks around 9°, 16°, 23°, 35°, and 41° (2θ)), C-S-H (peaks around 7° and 50° (2θ)) and hydrocalumite (Friedel's salt) (at 11° and 31° (2θ)) were identified

Rai reported a new phase formed in OPC retarded with 1.0wt% (74.6 mM) malic acid based on XRD analysis[17], but we did not find it. Moreover, the *d*-spacing of 3.235Å in Rai's results appears to be an error, with a true value being 3.352Å based on its 2θ value. As such, the peaks should be assigned to quartz (ICSD number 156196), which could be due to the contamination during the sample preparation. And the phase in the SEM BSE images in Rai's results could be ettringite, whose peaks in XRD results would easily be weakened or disappeared if the sample was hydration stopped.

3.2 Microstructure and morphology

After 11 years' hydration, there were still small amount of anhydrous cement particles remaining based on SEM results (Fig.2). Visually, the hydration products in the retarded paste had lower porosity and clearer boundaries between hydration products than those in the accelerated paste.

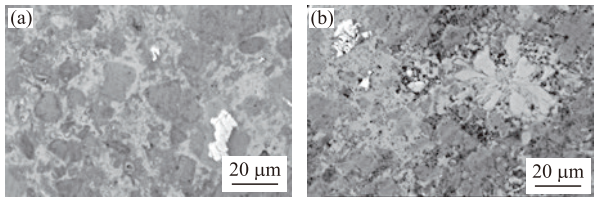

Fig.2 SEM BSE images of (a) retarded paste and (b) accelerated paste. There were still some anhydrous cement particle remains. Hydration products had clear boundaries and dense structures for the former while more porous in the latter

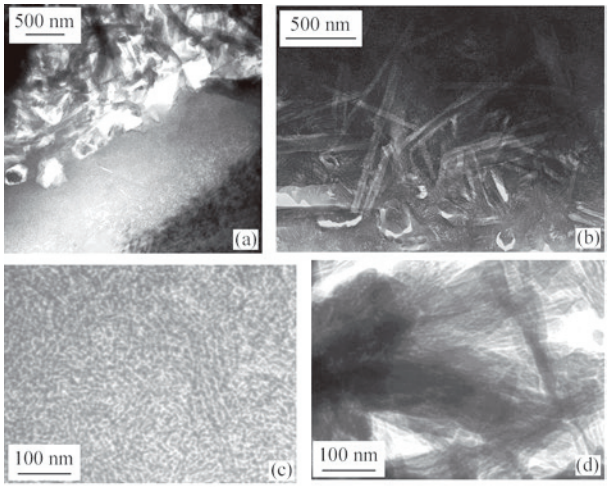

Fig.3 TEM images of WPC with 20 mM malic acid paste hydrated for 11 years: (a) Coarse Op C-S-H on the top, fine Ip C-S-H in the middle, CH in the left bottom corner and AFt relicts between Op and Ip C-S-H; (b) Needle-like AFt and AFt relicts in fine Ip C-S-H; (c) Detailed structure of Ip C-S-H; (d) Detailed structure of Op C-S-H

TEM images (Fig.3 and Fig.4) show that Op C-S-H was coarse fibrillar and Ip C-S-H was very fine in both pastes. In the retarded paste, there were some AFt relicts present at the interface between Ip and

Op C-S-H, and there was also some needle-like AFt within the fine Ip C-S-H, where the needle-like shape was due to the direction of the sample preparation[16]. In the accelerated paste, some AFt relicts were finely intermixed with Ip C-S-H. The particle size was about 7 nm for Ip C-S-H in both pastes. The particle size of Op C-S-H was about 5 nm in width in retarded paste while it was about 10-20 nm in accelerated paste. The finer microstructure of hydration products in the retarded paste may be due to that there is more time to get equilibrium in the system. For the different morphology in both pastes, they probably all had a similar underlying foil morphology, which was modified by drying or compacting during hydration stop or under vacuum[2]. The difference of appearance after drying was a result of different polymerisation degree (MCL) or porosity. For a longer MCL, the morphology tends to be foil-like or coarse fibrillar after drying due to better inter linking.

3.3 Chemical composition and nanostructure

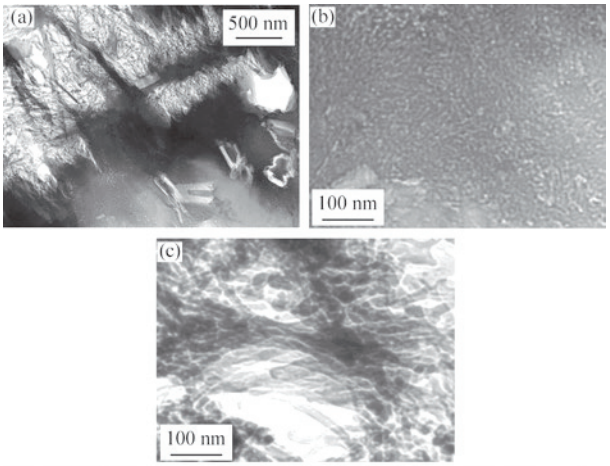

Fig.4 TEM images of WPC with 1 M calcium chloride paste hydrated for 11 years: (a) Coarse Op C-S-H on the top, fine Ip C-S-H on the bottom and AFt relicts and CH in the Ip C-S-H; (b) Detailed structure of Ip C-S-H; (c) Detailed structure of Op C-S-H

The formation of Portlandite, ettringite and C-S-H in both pastes and Friedel's salt in accelerated paste was also confirmed by STA-EGA analysis (Fig.5). There were two endotherms for both pastes around 100 ℃ and 450 ℃ in DTA curves associated with H_2O phases according to mass spectra. The former was due to the loss of water from C-S-H and ettringite; the latter from CH. A sharp exothermic peak around 650 ℃ was found, with some H_2O phases in the accelerated paste. It was thought to be related to a chloride C-S-H complex[3], and may be related to recrystallisation of Friedel's salt ($Ca_2Al(OH)_6Cl{\cdot}2H_2O$) to crystalline calcium chloroaluminate[18], $11CaO{\cdot}7Al_2O_3{\cdot}CaCl_2$. The calcium

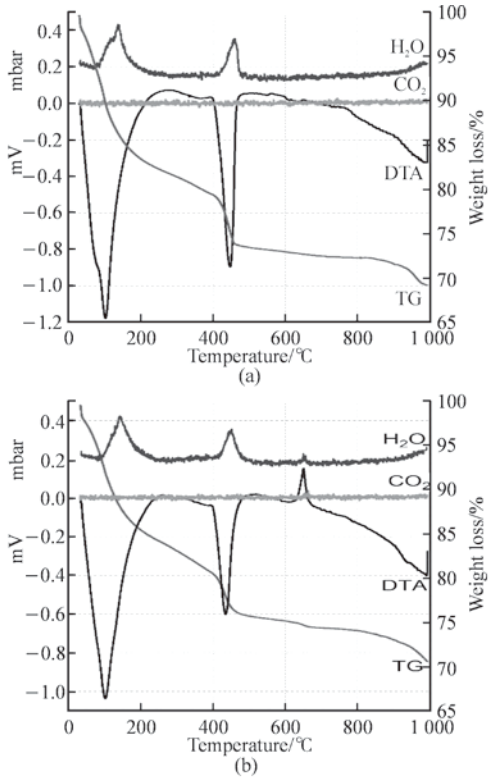

Fig.5 STA-EGA curves of (a) the retarded paste and (b) the accelerated paste. Paste was not carbonated. For the accelerated paste, the exothermic peak around 650 ℃ was due to the phase transformation from Friedel's salt ($Ca_2Al(OH)_6Cl{\cdot}2H_2O$) to crystalline calcium chloroaluminate ($11CaO{\cdot}7Al_2O_3{\cdot}CaCl_2$)

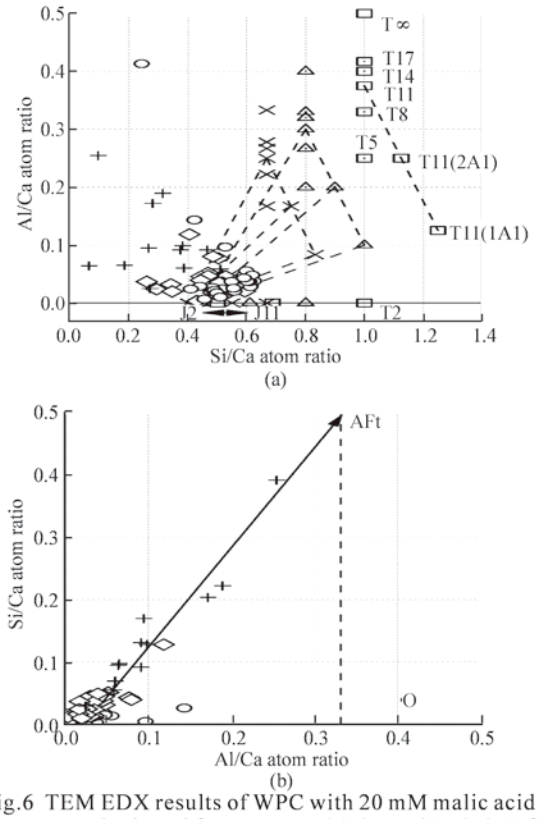

Fig.6 TEM EDX results of WPC with 20 mM malic acid paste hydrated for 11 years: (a) Op and Ip C-S-H fitted into T/J viewpoint; (b) AFt intermixed with C-S-H, no AFm was identified

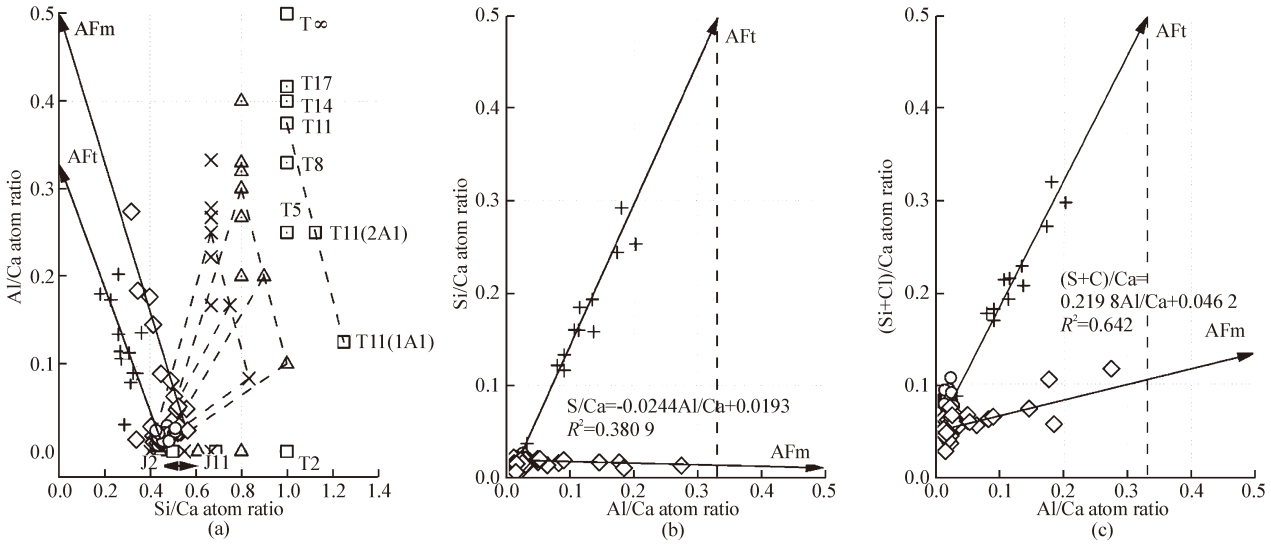

Fig.7 TEM EDX results of WPC with 1M calcium chloride paste hydrated for 11 years: (a) Ip and Op C-S-H fitted into T/J viewpoint; (b) AFt intermixed with C-S-H, and AFm intermixed with Op C-S-H; (c) Ip C-S-H had higher chloride content than Op C-S-H

Table 2 Chemical composition of C-S-H for WPC with 20mM malic acid paste and WPC with 1M calcium chloride paste both hydrated for 11 years, the Al/Si from NMR was under the condition that Q^{2B} was not taken into account

		Ca/Si	Al/Si (TEM)A	Al/Si$^{\triangle}$ (NMR)
Malic acid paste	Ip C-S-H (29*)	1.80 ± 0.16	0.055 ± 0.026	0.076
	Op C-S-H (35)	1.93 ± 0.20	0.054 ± 0.026	
Calcium chloride paste	Ip C-S-H (25)	2.14 ± 0.13	0.039 ± 0.011	0.076
	Op C-S-H (35)	2.14 ± 0.20	0.040 ± 0.013	

* Number of points performed TEM-EDX analysis; △ When Q^{2B} and Q^{2l} were not taken into account

Table 3 ^{29}Si SP MAS NMR results of both pastes with Q^{2B} taken into account. %B is percentage of bridging position occupied by aluminium tetrahedra in silicate/aluminium chain of C-S-H

	Percent reaction	MCL	Q^0(H)/%	Q^1 /%	Q^2(1Al)/%	Q^{2B}/%	Q^2 /%	Al/Si	B%/*
WPC with 20 mM malic acid	98.9	5.3	6.5	36.6	9.98	4.12	41.7	0.054	24.6
WPC with 1 M calcium chloride	100	7.0	5.8	28.0	7.54	6.86	51.9	0.040	16.1

* Percentage of bridging position occupied by aluminium tetrahedra in silicon/aluminum chain of C-S-H

hydroxide content in retarded paste and accelerated paste was 19.86% and 13.44%, respectively, which confirmed the XRD results. Cheeseman found that the content of calcium hydroxide was about 14% after 90 days hydration in OPC accelerated by 0.909 M calcium chloride paste[19]. Since both pastes were almost fully hydrated and the calcium hydroxide content of retarded paste was higher than that of accelerated paste, it is reasonable to predict that Ca/Si ratio of C-S-H in the former will be lower than that in the latter. This was confirmed by the TEM EDX results.

The TEM EDX results of both pastes are shown in Fig.6 and Fig.7. In these figures, squares indicate the different chain lengths of tobermorite or jennite structures which have a degree of protonation of the silicate chains (*w/n*) equalling 2; triangles are for a degree of protonation of the silicate chains equalling 1 and saltires (×) for a degree of protonation of the silicate chains equalling 0. The detailed discussion of these structures is in the Ref.[20]. Diamonds indicate outer products in the samples studied; circles indicate inner products and crosses indicate AFt or AFm. According to these results, AFt finely intermixed with C-S-H in both pastes and there was some low sulphate content AFm intermixed with Op C-S-H in accelerated paste, while no AFm was identified in retarded paste. For the accelerated paste, the chloride content in Ip C-S-H was higher than that in Op C-S-H, and there was some chloride incorporated into AFm phase, which could be in the form of Friedel's salt. The reason may be that chloride in the Op C-S-H existed in the form of Friedel's salt when Op C-S-H was formed first,

while chloride was just physically absorbed instead of chemically bonded in the Ip C-S-H later. The formula of AFm phase was calculated by fitting the trend line of mixtures of Op C-S-H and AFm phase as shown bellow: $[Ca_2Al(OH)_6]\cdot Cl_{0.312}\cdot(SO_4)_{0.028}\cdot(OH)_{0.66}\cdot mH_2O$.

Ca/Si and Al/Si ratios of these two pastes are shown in Table 2. C-S-H formed in WPC with 20 mM malic acid paste hydrated for 11 years and the sample had lower Ca/Si and higher Al/Si than that in WPC with 1M calcium chloride paste aged for 11 years, which confirmed the prediction from STA-EGA results.

^{29}Si CP and SP MAS NMR spectra and deconvoluted spectra are shown in Fig.8. On the top of the figures was the residue with zero line. The existence of various types of hydrated silicate tetrahedra could be identified by CP spectrum, and the quantity of these hydrated silicate tetrahedra could be calculated by deconvoluting the SP spectrum. According to the deconvoluted spectra, there was still small amount of anhydrous cement left in the retarded paste while the cement was fully hydrated in the accelerated paste. When the spectra were fitted to Q^0, Q^0(H), Q^1, Q^2(1Al) and Q^2, it was noticeable that Al/Si ratios from TEM and MAS NMR results were different: it was higher in the latter (Table 2). It was due to the possible extra peaks for Q^2 in ^{29}Si MAS NMR spectrum, namely Q^{2p} and Q^{2i} according to some researchers[21,22]. The peaks for Q^{2p} and Q^{2i} are -81.5×10^{-6} M and -83.5×10^{-6} M, respectively. The peak for Q^2(1Al) is around -82×10^{-6} M, which is very close to Q^{2p}. Q^{2p} and Q^{2i} are both silicate tetrahedra occupied on bridging sites but in the different local chemical environments. In this work, the peaks for Q^{2p} and Q^{2i} were taken into account during deconvoluting the spectrum. Q^{2p} was deconvoluted separately and Q^{2i} was treated as normal Q^2 during deconvolution because the peaks for Q^{2i} and Q^2 are so close that they overlap each other in which case it is not possible to distinguish them during deconvoluting, and it did not influence the Al/Si, MCL and %B whether Q^{2i} was deconvoluted separately. The condition whether or not Q^{2p} and Q^{2i} are taken into account during deconvoluting the spectrum will only influence the Al/Si ratio, MCL and %B of C-S-H. The method to introduce the additional Q^{2p} could be found in Taylor's paper[23], where it was named as Q^{2B}. In this paper, Q^{2p} will be named Q^{2B} when Q^{2i} was treated as a part of normal Q^2. In the case of existence of Q^{2p} and Q^{2i}, the results of ^{29}Si MAS NMR are shown in Table 2. There were Q^0(H), Q^1, Q^2(1Al), Q^{2B} and Q^2 in both pastes, but there were relatively less Q^1 and more Q^{2B} and Q^2 in WPC with the accelerated paste (Table 3), which resulted in a longer mean chain length (MCL) and less percentage of bridging tetrahedra occupied by aluminium (%B). Akhter[24] found that there was more Q^2 in C-S-H formed in OPC accelerated with 0.69 M to 2.64 M $CaCl_2$ in the pastes than those in OPC neat paste after 28 days hydration. It was noticed that the accelerated paste had longer MCL but also higher Ca/Si ratio, the reasons were that it had lower degree of protonation of silicate/aluminium chain in C-S-H and its nanostructure was combined by different types or/and amount of tobermorite/jennite units[20] comparing to the retarded paste.

The nanostructure and formula of C-S-H formed in both pastes could be achieved by combining the TEM and MAS NMR results. According to the Al/Ca - Si/Ca plots of both samples, the nanostructure of C-S-H could be well fit into tobermorite/jennite (T/J) model. The method to establish formula and identify the nanostructure of C-S-H could be found in some recent

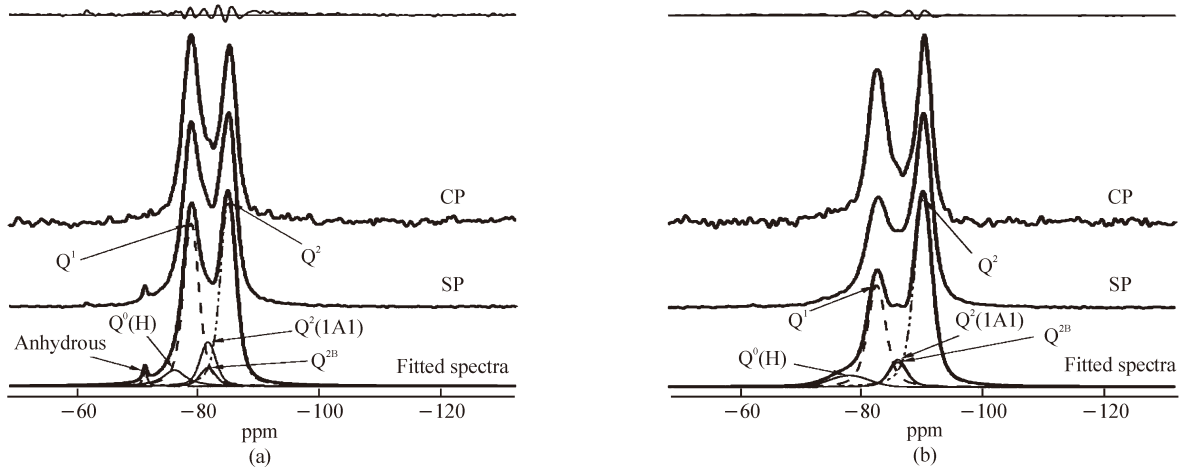

Fig.8 ^{29}Si MAS NMR results of both samples: (a) WPC with 20 mM malic acid paste hydrated for 11 years; (b) WPC with 1 M calcium chloride paste hydrated for 11 years

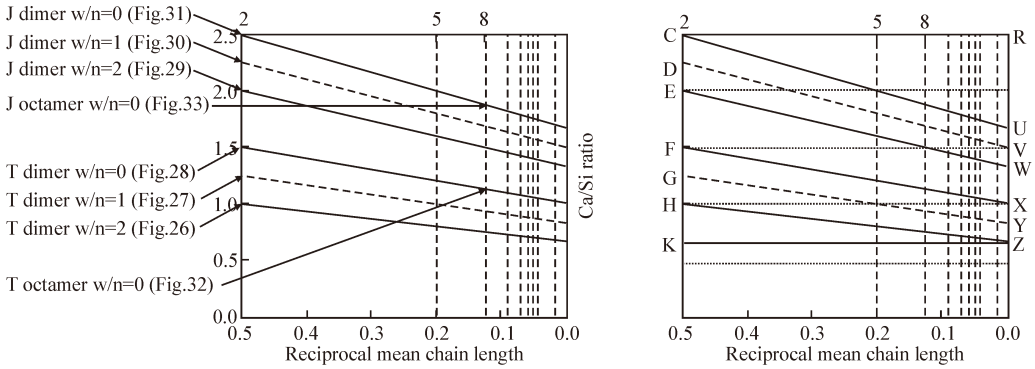

Fig.9 Relationship between Ca/Si ratio and MCL for structure units with different degree of protonation of the silicate chains (*w/n*=0, 1, and 2) modified from Richardson's model[20]

studies[20, 27-29]. Al/Si ratio from TEM was used during calculating the formula because of the inaccuracy of Al/Si from NMR discussed above. According to Richardson's model[20, 30, 31], the chemical composition of C-S-H has a strong relationship with the nanostructure (T/CH or T/J viewpoint) but this is not the only factor, as the degree of protonation will influence the chemical composition of C-S-H. As seen in Fig. 9, for a jennite-based dimer, the Ca/Si ratio can vary from 2.0 to 2.5 with the degree of protonation of silicate chains varying from 2 to 0, being the maximum and minimum. This is due to the fact that for a given MCL, the Ca/Si ratio can vary largely under the condition of different combination of tobermorite/jennite units and degree of protonation of silicate chains in these units. That means a longer MCL will not necessarily have a lower Ca/Si ratio. Every combination of a MCL and a Ca/Si ratio for C-S-H could be shown as a point in Fig.9, but these points will not be restricted in the C-U-Z-H area but have to be within the C-R-Z-K area.

Because there were only trace amount of K_2O and Na_2O in WPC used in this work, it could be assumed that the charge compensation of Al^{3+} substituting for Si^{4+} was entirely balanced by Ca^{2+}. The degree of protonation could vary from minimum to maximum for C-S-H, which will be discussed in detail later. For the retarded paste, the formulae under both conditions were shown below.

The formula of Ip C-S-H under the minimum degree of protonation of silicate chains would be:

$$\{Ca_{4.215}(Si_{0.948}Al_{0.052})_{5.3}O_{17.0}\}Ca_{0.138} \cdot (OH)_{5.27} \cdot Ca_{4.7} \cdot mH_2O\} \quad (1)$$

The formula of Ip C-S-H under the maximum degree of protonation of silicate chains (according to the calculation) would be:

$$\{Ca_{4.215}H_{3.161}(Si_{0.948}Al_{0.052})_{5.3}O_{17.0}\}Ca_{0.138} \cdot (OH)_{8.43} \cdot Ca_{4.7} \cdot mH_2O\} \quad (2)$$

The formula of Op C-S-H under the minimum degree of protonation of silicate chains would be:

$$\{Ca_{4.2}(Si_{0.948}Al_{0.051})_{5.3}O_{16.9}\}Ca_{0.136} \cdot (OH)_{6.57} \cdot Ca_{5.38} \cdot mH_2O\} \quad (3)$$

The formula of Op C-S-H under the maximum degree of protonation of silicate chains (according to the calculation) would be:

$$\{Ca_{4.2}H_{1.83}(Si_{0.949}Al_{0.051})_{5.3}O_{16.9}\}Ca_{0.136} \cdot (OH)_{8.4} \cdot Ca_{5.38} \cdot mH_2O\} \quad (4)$$

For the accelerated paste, as there were a large amount of Ca^{2+} cations in the solution, it could be assumed that C-S-H nanostructure had a minimum degree of protonation of silicate chains (*w/n*=0). Under this condition, the formulae of Ip C-S-H would be:

$$\{Ca_{5.3331}(Si_{0.963}Al_{0.037})_{7.0}O_{22.0}\}Ca_{0.131} \cdot (OH)_{12.52} \cdot Ca_{8.9} \cdot mH_2O\} \quad (5)$$

$$\{Ca_{5.337}(Si_{0.961}Al_{0.039})_{7.0}O_{22.0}\}Ca_{0.135} \cdot (OH)_{12.53} \cdot Ca_{8.9} \cdot mH_2O\} \quad (6)$$

To determine the protonation of silicate chains of C-S-H in the pastes, the Ca/(Si+Al)-MCL plots with Ca/(Si+Al) ratio frequency histogram (Fig. 10 and Fig.11) were used to give an idea of the possible degree of protonation of silicate chains in C-S-H nanostructure. The Ca/(Si+Al) ratio instead of Ca/Si was used here because the percentages of bridging tetrahedra occupied by Al were high and could influence the position of tobermorite-type units in the plots according to the ^{29}Si

SP MAS NMR results. The alternative lines, which are not presented in Fig.9, presented the position of jennite units or tobermorite units under the condition that the charges caused by Al^{3+} ions substituting for Si^{4+} ions in bridging tetrahedra were entirely balanced by Ca^{2+}.

In these plots (Fig.10 and Fig.11), the vertical black lines represent the MCL of the silicate/aluminium chains, and the histogram shows the Ca/(Si+Al) ratio frequency of the TEM-EDX results of the points analysed. These plots could also give a possible combination of tobermorite and/or jennite units on which the nanostructure of C-S-H is based.

For the retarded paste, the Ip C-S-H consisted of J5, J8, T5, and T8, and maybe some J2 and T2. J2, J5, and J8 should have minimum to maximum degree of protonation of silicate chains. T2, T5, and T8 should have minimum degree of protonation of silicate/aluminium chains and the charges caused by Al^{3+} for substituting for Si^{4+} ions were completely balanced by Ca^{2+}. In this case, a near medium degree of protonation could be chosen for Ip C-S-H. Let *w/n*=1, which is the condition of medium degree of protonation, the following formula would present the nanostructure and chemical composition of Ip C-S-H in the retarded paste:

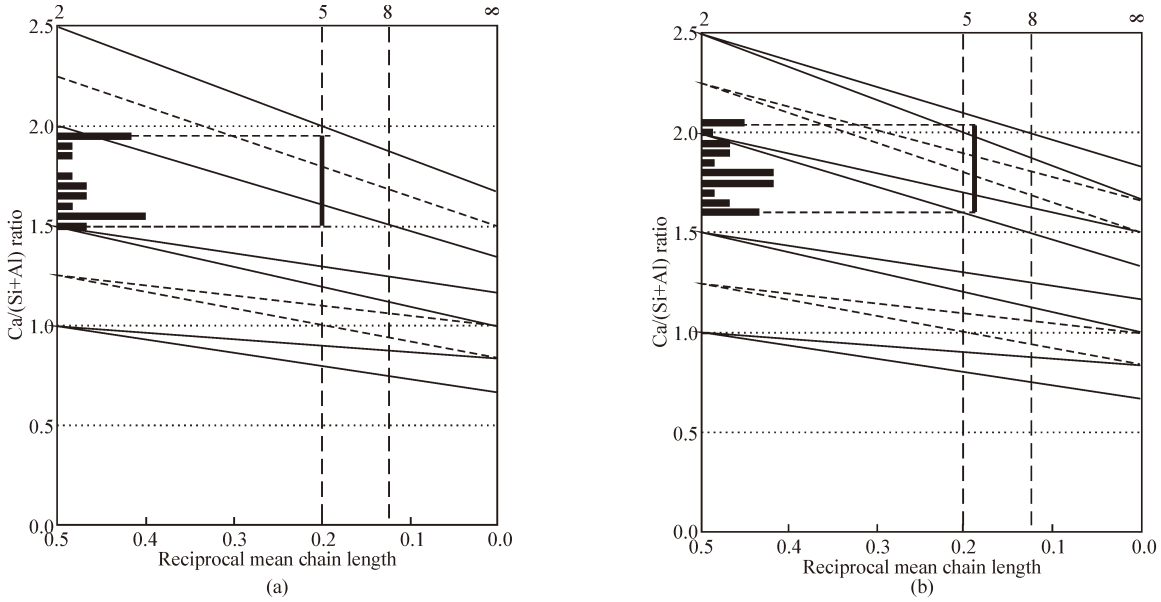

Fig.10 Ca/(Si+Al)-MCL plot with Ca/(Si+Al) ratio frequency histogram of TEM-EDX results of (a) Ip and (b) Op C-S-H of WPC with 20mM malic acid paste hydrated for 11 years

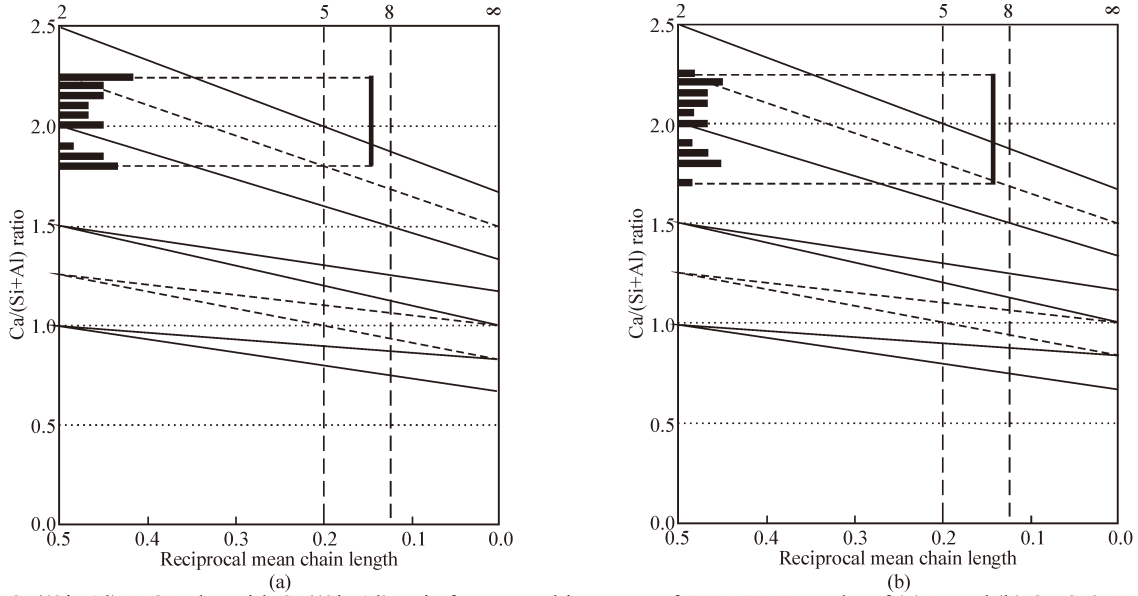

Fig.11 Ca/(Si+Al)-MCL plot with Ca/(Si+Al) ratio frequency histogram of TEM-EDX results of (a) Ip and (b) Op C-S-H of WPC with 1M calcium chloride paste hydrated for 11 years

$$\{Ca_{4.215}H_{2.107}(Si_{0.948}Al_{0.052})_{5.3}O_{17.0}\}Ca_{0.138} \cdot (OH)_{6.46} \cdot Ca_{4.7} \cdot mH_2O\} \quad (7)$$

The Op C-S-H consisted of J2, J5, J8, T5, T8 and maybe T2. J2, J5, and J8 should have minimum to maximum degree of protonation of silicate chains. T5 and T8 should have minimum degree of protonation of silicate chains and the charges caused by Al^{3+} ions substituting for Si^{4+} ions were completely balanced by Ca^{2+}. In this case, a near medium degree of protonation of silicate chains could be chosen for Op C-S-H. Because the possible maximum protonation is w/n=0.85, Formula 4 could well present the nanostructure and chemical composition of Op C-S-H in the retarded paste.

For the accelerated paste, Ip and Op C-S-H should both consist of J2, J5, J8, T5, T8 and maybe T2. J2, J5, and J8 should have minimum to maximum degree of protonation of silicate chains. T5 and T8 should have minimum degree of protonation of silicate chains and the charges caused by Al^{3+} ions substituting for Si^{4+} ions were completely balanced by Ca^{2+}. The degree of protonation discussed above was mean value, the nanostructure and chemical composition could vary depending on the local environment.

4 Conclusions

The hydration products of WPC with 20 mM malic acid paste hydrated for 11 years were CH, ettringite and C-S-H. It was similar for WPC with 1 M calcium chloride paste hydrated for 11 years but with less CH, and the formation of Friedel's salt ($Ca_2Al(OH)_6Cl{\cdot}2H_2O$). SEM results showed that there were still small amount of anhydrous cement particles remaining in both pastes after 11 years hydration, which were confirmed by the ^{29}Si MAS NMR results. It seems that the hydration products of WPC with 20 mM malic acid paste had lower porosity upon visual inspection, which may be due to the better equilibrium. The morphology of Op C-S-H was coarse fibrillar and Ip C-S-H had very fine structure in both pastes according to the TEM results. There were some AFt relicts present at the interface between Ip and Op C-S-H and some needle-like AFt in fine Ip C-S-H in WPC with 20 mM malic acid paste, while some AFt relicts were finely intermixed with Ip C-S-H and AFm intermixed with Op C-S-H in WPC with 1 M calcium chloride paste. Ip C-S-H particle size was about 7 nm in both pastes, while Op C-S-H particle size was about 5 nm in width in malic acid paste and 10-20 nm in calcium chloride paste. It seems that the accelerated hydration with a faster hydration speed results in less equilibrium so as to a microstructure of coarser hydration products and lower density.

AFt was finely intermixed with C-S-H in both pastes and there was some low sulphate content AFm intermixed with Op C-S-H in the accelerated paste while no AFm was identified in the retarded paste. Both Ip and Op C-S-H formed in the retarded paste had lower Ca/Si and higher Al/Si than that in the accelerated paste. There were Q^0(H), Q^1, Q^2(1Al), Q^2B and Q^2 in both pastes, however there were relatively less Q^1 and more Q^{2B} and Q^2 in the accelerated paste, which resulted in a longer mean chain length (MCL) and less percentage of bridging tetrahedra occupied by aluminium (%B). The accelerated paste had longer MCL but also higher Ca/Si ratio because it had lower degree of protonation of silicate/aluminium chain in C-S-H and its nanostructure was combined by different types or/and amount of tobermorite/jennite units comparing to the retarded paste. This indicates that a longer MCL does not mean a lower Ca/Si ratio when comparing different pastes.

References

[1] Richardson IG. The Calcium Silicate Hydrates [J]. *Cement and Concrete Research*, 2008,38: 137-158

[2] Taylor HFW. *Cement Chemistry*[M]. London: Thomas Telford Services Ltd., 1997

[3] Traetteberg A, Ramachandran VS, Grattan-Bellew PE. A Study of the Microstructure and Hydration Characteristics of Tricalcium Silicate in the presence Of Calcium Chloride [J]. *Cement and Concrete Research*, 1974,4: 203-221

[4] Collepardi M, Marchese B. Morphology and Surface Properties of Hydrated Tricalcium Silicate Pastes [J]. *Cement and Concrete Research*, 1972, 2:57-65

[5] Young JF, Berger RL, FVL Jr. Studies on The Hydration of Tricalcium Silicate Pastes: III. Influence of Admixtures on Hydration and Strength Development [J]. *Cement and Concrete Research*, 1973,3: 689-700

[6] Groves GW, LeSueur PJ, Sinclair W. Transmission Electron Microscopy and Microanalystical Studies of Ion-Beam-Thinned Sections of Tricalcium Silicate Paste [J]. *J. Am. Ceram. Soc*., 1986,89: 353-356

[7] Juenger MCG, Jennings HM. The Use of Nitrogen Adsorption to Assess the Microstructure of Cement Pastes [J]. *Cement and Concrete Research*, 2001, 31: 883-892

[8] Juenger MCG, Monteiro PJM, Gartner EM, *et al*. Soft X-ray Microscope Investigation into the Effects of Calcium Chloride on Tricalcium Silicate Hydration [J]. *Cement and Concrete Research*, 2005, 35: 19-25

[9] Peterson VK, Juenger MCG. Time-Resolved Quasielastic Neutron Scattering Study of the Hydration of Tricalcium Silicate: Effects of $CaCl_2$ and Sucrose [J]. *Physica B-Condensed Matter*, 2006, 385: 222-224

[10] Wilding CR, Walter A, Double DD. A Calssification of Inorganic and Organic Admixtures by Conduction Calorimetry [J]. *Cement and Concrete Research*, 1984, 14: 185-194

[11] Brough AR, Holloway M, Sykes J, *et al.* Sodium Silicate-Based Alkali-Activated Slag Mortars Part II. The Retarding Effect of Additions of Sodium Chloride or Malic Acid [J]. *Cement and Concrete Research*, 2000, 20: 1 375-1 379

[12] Ersen A, Smith A, Chotard T. Effect of Malic and Citric Acid on the Crystallisation of Gypsum Investigated by Coupled Acoustic Emission And Electrical Conductivity Techniques [J]. *Journal of Materials Science*, 2006, 41: 7 210-7 217

[13] Wang XP, Ye JD, Wang YJ. Effect of Additives on the Morphology of the Hydrated Product and Physical Properties of a Calcium Phosphate Cement [J]. *Journal of Materials Science & Technology*, 2008, 24: 285-288

[14] Rai S, Chaturvedi S, Singh NB. Examination of Portland Cement Paste Hydrated in the Presence of Malic Acid [J]. *Cement and Concrete Research*, 2004, 34: 455-462

[15] Brough AR. *NMR Studies of Inorganic Solids*[D]. Oxford: University of Oxford, 1993

[16] Richardson IG, Groves GW. Microstructure and Microanalysis of Hardened Ordinary Portland Cement Pastes [J]. *Journal of Materials Science*, 1993, 28: 265-277

[17] Rai S, Chaturvedi S, Singh H. Examination of Portland Cement Paste Hydrated in the Presence of Malic Acid [J]. *Cement and Concrete Research*, 2004, 34: 455-462

[18] Birnin-Yauri UA, Glasser FP. Friedel's salt, $Ca_2Al(OH)_6(Cl,OH)\ 2H_2O$: Its Solid Solutions and Their Role in Chloride Binding [J]. *Cement and Concrete Research*, 1998, 28: 1 713-1 723

[19] Cheeseman CR, Asavapisit S. Effect of Calcium Chloride on the Hydration and Leaching of Lead-Retarded Cement [J]. *Cement and Concrete Research*, 1999, 29: 885-892

[20] Richardson IG. Tobermorite/jennite- and Tobermorite/calcium Hydroxide-Based Models for the Structure of C-S-H: Applicability to Hardened Pastes of Tricalcium Silicate, Beta-Dicalcium Silicate, Portland Cement, and Blends of Portland Cement With Blast-Fumace Slag, Metakaolin, or Silica Fume [J]. *Cement and Concrete Research*, 2004, 34: 1 733-1 777

[21] Klur I, Jacquinot JF, Brunet F, *et al.* NMR Cross-Polarization When TIS>T1p; Examples From Silica Gel and Calcium Silicate Hydrates [J]. *J. Phys. Chem. B*, 2000, 104: 10 162-10 167

[22] Brunet F, Bertani P, Charpentier T, *et al*. Application of ^{29}Si Homonuclear and ^{1}H-^{29}Si Heteronuclear NMR Correlation to Structural Studies of Calcium Silicate Hydrates [J]. *Journal of Physical Chemistry B*, 2004, 108: 15 494-15 502

[23] Taylor R, Richardson IG, Brydson RMD. Composition and Microstructure of 20-Year-Old Ordinary Portland Cement-Ground Granulated Blast-Furnace Slag Blends Containing 0 to 100% Slag [J]. *Cement and Concrete Research*, 2010, 40: 971-983

[24] Akhter H, Cartledge FK, Roy A, *et al.* A Study of the Effects of Nickel Chloride and Calcium Chloride on the Hydration of Portland Cement [J]. *Cement and Concrete Research*, 1993, 23: 833-842

[25] Rodger SA. *The Chemistry of Admixture Interaction During Cement Hydration*[M]. Oxford: Department of Materials, University of Oxford, 1986

[26] Andersen MD, Jakobsen HJ, Skibsted J. Characterization of White Portland Cement Hydration and the C-S-H Structure in the Presence of Sodium Aluminate by 27Al and ^{29}Si MAS NMR Spectroscopy [J]. *Cement and Concrete Research*, 2004,34: 857-868

[27] Love CA, Richardson IG, Brough AR. Composition and Structure of C-S-H in White Portland Cement-20% Metakaolin Pastes Hydrated at 25 ℃[J]. *Cement and Concrete Research*, 2007, 37: 109-117

[28] Girao AV, Richardson IG, Porteneuve CB, *et al*. Composition, Morphology and Nanostructure of C-S-H in White Portland Cement-Fly Ash Blends Hydrated at 85 ℃[J]. *Adv. Appl. Ceram.*, 2007,106: 283-293

[29] Taylor R, Richardson IG, Brydson R. Nature of C-S-H in 20 Year Old Neat Ordinary Portland Cement and 10% Portland Cement-90% Ground Granulated Blast Furnace Slag Pastes[J]. *Adv. Appl. Ceram*., 2007, 106: 294-301

[30] Richardson IG, Groves GW. Models for the Composition and Structure of Calcium Silicate Hydrate (C-S-H) Gel in Hardened Tricalcium Silicate Pastes [J]. *Cement and Concrete Research*, 1999, 22: 1 001-1 010

[31] Richardson IG, Groves GW. The Incorporation of Minor and Trace-Elements into Calcium Silicate Hydrate (C-S-H) Gel in Hardened Cement Pastes [J]. *Cement and Concrete Research*, 1993, 23: 131-138